The environment of pulsar halo progenitors

Lioni-Moana Bourguinat
Carmelo Evoli, Pierrick Martin, Sarah Recchia

GRAN SASSO SCIENCE INSTITUTE
SCHOOL OF ADVANCED STUDIES
Scuola Universitaria Superiore
INFN

Geminga as seen by Chandra and Spitzer
Credits: X-ray: NASA/CXC/PSU/B. Posselt et al; Infrared: NASA/JPL-Caltech

TeV Halos

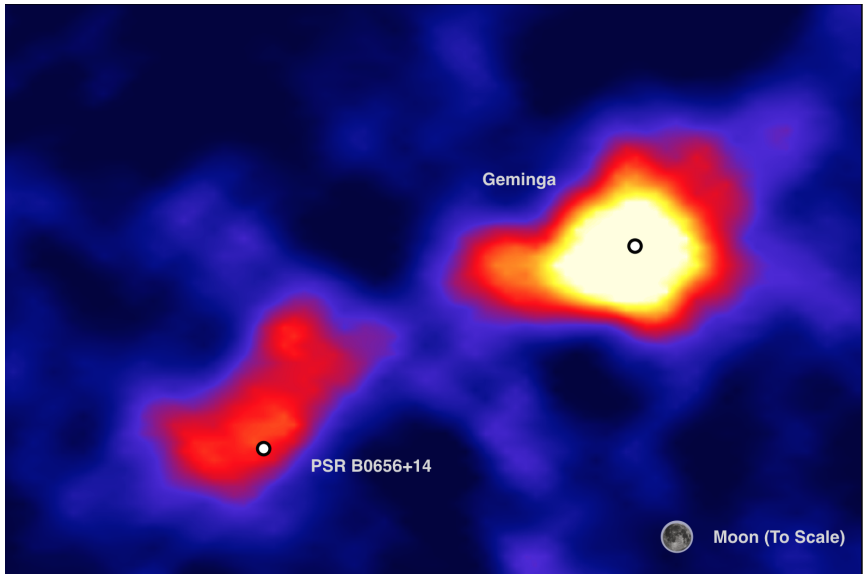

Figure: HAWC sky map of TeV emission from Geminga and its neighbour PSR B0656+14.
Credits: HAWC Collaboration

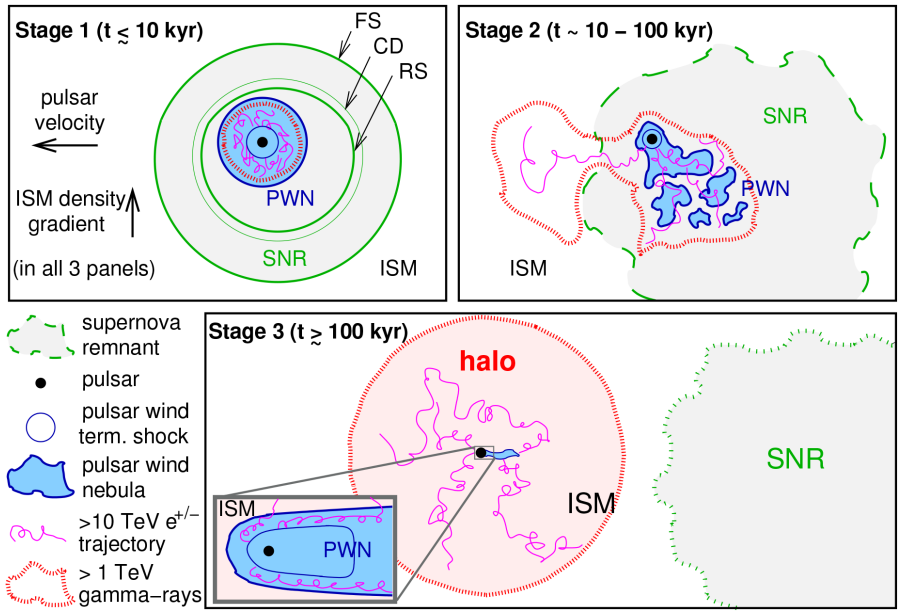

Figure: Sketch of the main evolutionary stages of a pulsar wind nebula.
Credits: Giacinti et al. (2020)

TeV Halos

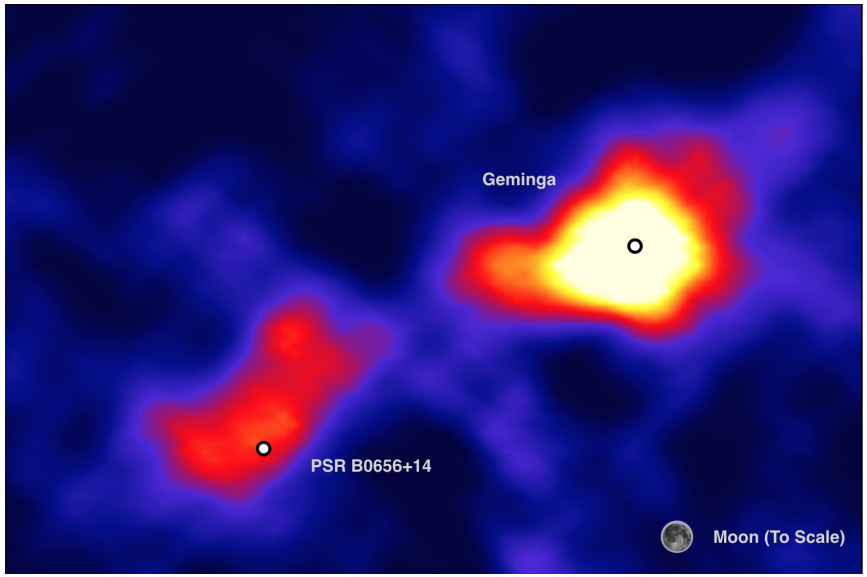

Figure: HAWC sky map of TeV emission from Geminga and its neighbour PSR B0656+14.
Credits: HAWC Collaboration

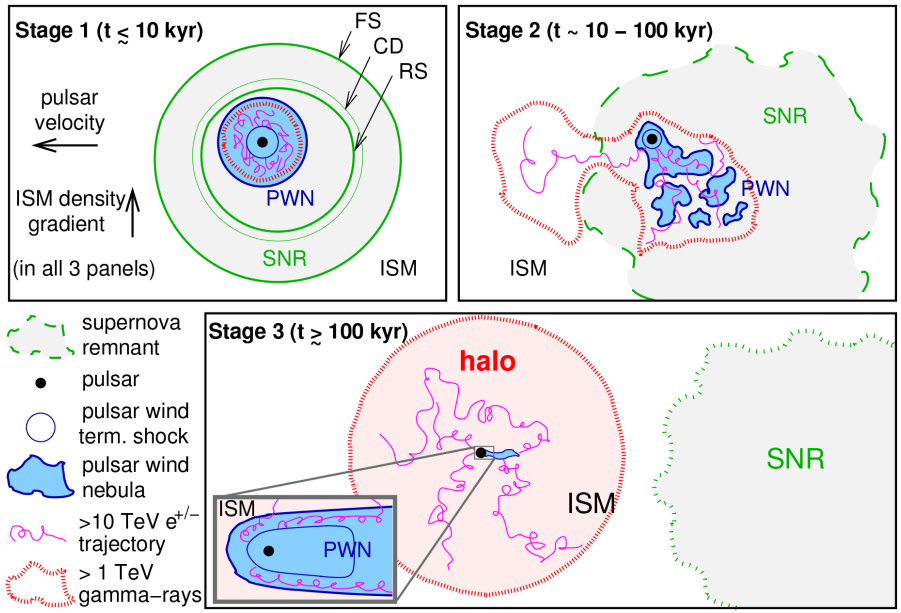

Figure: Sketch of the main evolutionary stages of a pulsar wind nebula.
Credits: Giacinti et al. (2020)

Standard assumption

Pulsar **outside** the SNR → Low diffusion coefficient problem [Abeysekara et al. (2017)]

Solving the diffusion coefficient problem

Theoretical explanations

- Cosmic-ray pairs induced turbulence [Evoli, Linden, et al. (2018), Mukhopadhyay et al. (2022)]
- **Environment induced turbulence** [Fang et al. (2019), Schroer et al. (2022)]

Solving the diffusion coefficient problem

Theoretical explanations

- Cosmic-ray pairs induced turbulence [Evoli, Linden, et al. (2018), Mukhopadhyay et al. (2022)]
- **Environment induced turbulence** [Fang et al. (2019), Schroer et al. (2022)]

Which medium are the leptons probing when we see a TeV halo?

Solving the diffusion coefficient problem

Theoretical explanations

- Cosmic-ray pairs induced turbulence [Evoli, Linden, et al. (2018), Mukhopadhyay et al. (2022)]
- **Environment induced turbulence** [Fang et al. (2019), Schroer et al. (2022)]

Which medium are the leptons probing when we see a TeV halo?

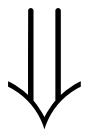

Where is the pulsar at a given age?

Goal of this work

Method

Computation of the escape time from the SNR and bubble of a population of pulsars using a Monte Carlo approach for 3 models:

- ISM (interstellar medium) Physically irrelevant!!
- IMSB (isolated massive star bubble)
- SB (superbubble)

Property of the pulsars: Kick velocity

Kick velocity distribution

Taken from Faucher-Giguère et al. (2006), modulus of all components:

$$f(v_{\rm k}^{x,y,z}) = w\,\mathcal{N}(v_{\rm k}, \sigma = 160 \text{ km/s}) + (1-w)\,\mathcal{N}(v_{\rm k}, \sigma = 780 \text{ km/s}) \quad (1)$$

with $w = 0.90$.

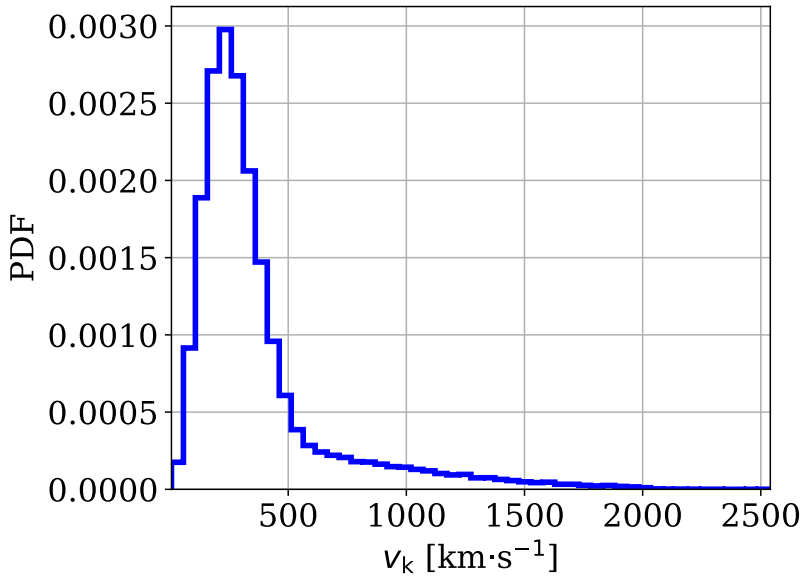

Figure: PDF of the kick velocity of pulsars.

Isolated massive star bubble model

Assumptions

- CC SN happens in the **isolated massive star bubble** shaped by the progenitor
- The SNR is stopped by the bubble shell.

Isolated massive star bubble model

Assumptions

- CC SN happens in the **isolated massive star bubble** shaped by the progenitor
- The SNR is stopped by the bubble shell.

Process

- Pick a random **progenitor mass** from a Galactic Initial Mass Function (IMF) with $[8; 40]$ $M_\odot$,
- **Star properties** [Seo et al. (2018)],
- **Bubble properties** [Weaver et al. (1977), Härer et al. (2023)].

Neglecting post-MS phases for the wind and bubble structure.

Isolated massive star bubble model

Assumptions

- CC SN happens in the **isolated massive star bubble** shaped by the progenitor
- The SNR is stopped by the bubble shell.

Process

- Pick a random **progenitor mass** from a Galactic Initial Mass Function (IMF) with $[8; 40]$ $M_\odot$,
- **Star properties** [Seo et al. (2018)],
- **Bubble properties** [Weaver et al. (1977), Härer et al. (2023)].

Neglecting post-MS phases for the wind and bubble structure.

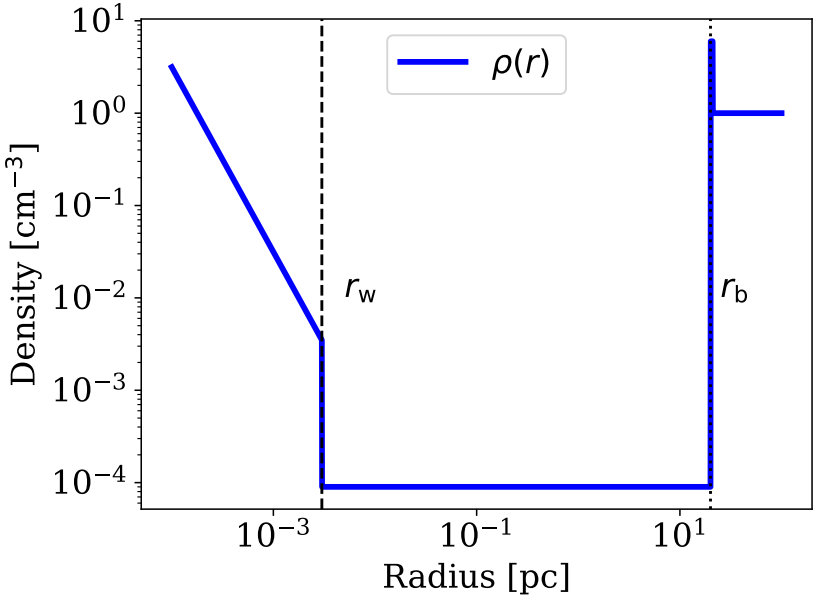

Figure: Density profile in the IMSB, based on Weaver et al. (1977).

Superbubble model

Assumptions

- Point-like cluster/OB association surrounded by a **superbubble** [Weaver et al. (1977)]
- Ambient density of $n_{\mathrm{ISM}} \sim 100\ \mathrm{cm}^{-3}$ [Parizot et al. (2004)]
- The SNR merges within the SB [Mac Low et al. (1988)]

Superbubble model

Assumptions

- Point-like cluster/OB association surrounded by a **superbubble** [Weaver et al. (1977)]
- Ambient density of $n_{\mathrm{ISM}} \sim 100\ \mathrm{cm}^{-3}$ [Parizot et al. (2004)]
- The SNR merges within the SB [Mac Low et al. (1988)]

Process

Pick a **random cluster mass** following a cluster IMF [Portegies Zwart et al. (2010)].

Populate with stars following the Galactic IMF.

Compute the **cluster luminosity** and SB radius [Weaver et al. (1977), Härer et al. (2023)].

Pick a **random massive star** and find the associated MS time [Seo et al. (2018)].

Creation of a pulsar at the MS time and propagation of both pulsar and SB radius.

Probabilities of finding isolated massive stars

Isolated massive star formation

Massive stars are created in groups [Wright (2020)].

Runaway stars

The runaway probabilities are [Zinnecker et al. (2007)]:

- 2% of **B** stars,
- 25% of **O** stars.

Star masses are taken between $8\ \mathrm{M}_\odot < M_\star < 40\ \mathrm{M}_\odot$.

Probabilities of finding isolated massive stars

Isolated massive star formation

Massive stars are created in groups [Wright (2020)].

Runaway stars

The runaway probabilities are [Zinnecker et al. (2007)]:

- 2% of **B** stars,
- 25% of **O** stars.

Star masses are taken between $8\ \mathrm{M}_\odot < M_\star < 40\ \mathrm{M}_\odot$.

$\rightarrow$ 10% of **IMSB**, 90% of **SB**.

Comparing the probability of being inside the boundary

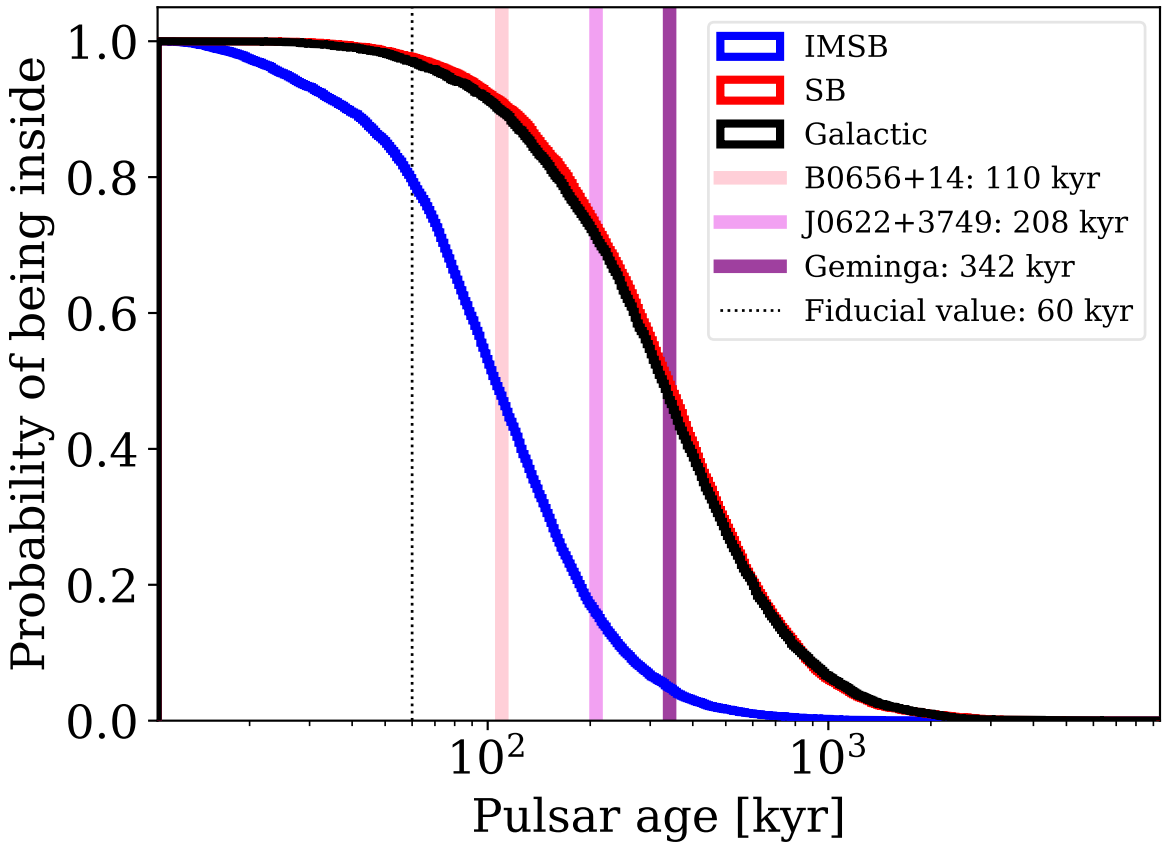

Figure: Probability of pulsars being inside the boundary as a function of time for **IMSB**, **SB** and **Galactic** pulsar populations.
Characteristic ages of pulsars are orders of magnitude, taken from the catalog of Manchester et al. (2005).

Some numbers

Pulsar	Age [kyr]	Inside (IMSB)	Inside (SB)	Inside (Gal)
B0656+14	110	48%	91%	90%
J0622+3749	208	16%	73%	71%
Geminga	342	5%	49%	48%

Some numbers

Pulsar	Age [kyr]	Inside (IMSB)	Inside (SB)	Inside (Gal)
B0656+14	110	48%	91%	90%
J0622+3749	208	16%	73%	71%
Geminga	342	5%	49%	48%

More on Geminga

Hints that Geminga is in a hot ionized medium:

- No H_α lines in the near vicinity [Caraveo et al. (2003)]
- Proximity to Gemini H_α Ring bubble [Knies et al. (2018)]

Summary

Main questions

Which medium are the leptons probing when we see a TeV halo?
Where is the pulsar at a given age?

Summary

Main questions

Which medium are the leptons probing when we see a TeV halo?
Where is the pulsar at a given age?

Conclusions

- Typically assumed: ~ 50 kyr and probe the ISM.
- We find instead a majority of $\gtrsim$ **100 kyr pulsars are inside the IMSB/SB**.
- Are Geminga and PSR B0656+14 in a **hot and turbulent** environment?
- How are IMSB/SB connected to **TeV halos**?
- How about similar pulsars in **radio**?

Thank you for your attention!

Bibliography I

Abeysekara, A. U. et al. (Nov. 2017). "Extended gamma-ray sources around pulsars constrain the origin of the positron flux at Earth". In: *Science* 358.6365, pp. 911–914. DOI: 10.1126/science.aan4880. arXiv: 1711.06223 [astro-ph.HE].

Caraveo, P. A. et al. (Sept. 2003). "Geminga's Tails: A Pulsar Bow Shock Probing the Interstellar Medium". In: *Science* 301.5638, pp. 1345–1348. DOI: 10.1126/science.1086973.

Cioffi, Denis F. et al. (Nov. 1988). "Dynamics of Radiative Supernova Remnants". In: ApJ 334, p. 252. DOI: 10.1086/166834.

Evoli, Carmelo, Elena Amato, et al. (Apr. 2021). "Galactic factories of cosmic-ray electrons and positrons". In: Phys. Rev. D 103.8, 083010, p. 083010. DOI: 10.1103/PhysRevD.103.083010. arXiv: 2010.11955 [astro-ph.HE].

Evoli, Carmelo, Tim Linden, et al. (Sept. 2018). "Self-generated cosmic-ray confinement in TeV halos: Implications for TeV γ -ray emission and the positron excess". In: Phys. Rev. D 98.6, 063017, p. 063017. DOI: 10.1103/PhysRevD.98.063017. arXiv: 1807.09263 [astro-ph.HE].

Fang, Kun et al. (Sept. 2019). "Possible origin of the slow-diffusion region around Geminga". In: MNRAS 488.3, pp. 4074–4080. DOI: 10.1093/mnras/stz1974. arXiv: 1903.06421 [astro-ph.HE].

Faucher-Giguère, Claude-André and Victoria M. Kaspi (May 2006). "Birth and Evolution of Isolated Radio Pulsars". In: ApJ 643.1, pp. 332–355. DOI: 10.1086/501516. arXiv: astro-ph/0512585 [astro-ph].

Giacinti, G. et al. (Apr. 2020). "Halo fraction in TeV-bright pulsar wind nebulae". In: A&A 636, A113, A113. DOI: 10.1051/0004-6361/201936505. arXiv: 1907.12121 [astro-ph.HE].

Härer, Lucia K. et al. (Mar. 2023). "Understanding the TeV γ-ray emission surrounding the young massive star cluster Westerlund 1". In: A&A 671, A4, A4. DOI: 10.1051/0004-6361/202245444. arXiv: 2301.10496 [astro-ph.HE].

Bibliography II

Knies, Jonathan R. et al. (July 2018). "Suzaku observations of the Monogem Ring and the origin of the Gemini H α ring". In: MNRAS 477.4, pp. 4414–4422. DOI: 10.1093/mnras/sty915.

Leahy, D. A., S. Ranasinghe, et al. (May 2020). "Evolutionary Models for 43 Galactic Supernova Remnants with Distances and X-Ray Spectra". In: ApJS 248.1, 16, p. 16. DOI: 10.3847/1538-4365/ab8bd9. arXiv: 2003.08998 [astro-ph.HE].

Leahy, D. A. and J. E. Williams (May 2017). "A Python Calculator for Supernova Remnant Evolution". In: AJ 153.5, 239, p. 239. DOI: 10.3847/1538-3881/aa6af6. arXiv: 1701.05942 [astro-ph.HE].

Mac Low, Mordecai-Mark and Richard McCray (Jan. 1988). "Superbubbles in Disk Galaxies". In: ApJ 324, p. 776. DOI: 10.1086/165936.

Manchester, R. N. et al. (Apr. 2005). "The Australia Telescope National Facility Pulsar Catalogue". In: AJ 129.4, pp. 1993–2006. DOI: 10.1086/428488. arXiv: astro-ph/0412641 [astro-ph].

Mukhopadhyay, Payel and Tim Linden (June 2022). "Self-generated cosmic-ray turbulence can explain the morphology of TeV halos". In: Phys. Rev. D 105.12, 123008, p. 123008. DOI: 10.1103/PhysRevD.105.123008. arXiv: 2111.01143 [astro-ph.HE].

Parizot, E. et al. (Sept. 2004). "Superbubbles and energetic particles in the Galaxy. I. Collective effects of particle acceleration". In: A&A 424, pp. 747–760. DOI: 10.1051/0004-6361:20041269. arXiv: astro-ph/0405531 [astro-ph].

Portegies Zwart, Simon F. et al. (Sept. 2010). "Young Massive Star Clusters". In: ARA&A 48, pp. 431–493. DOI: 10.1146/annurev-astro-081309-130834. arXiv: 1002.1961 [astro-ph.GA].

Schroer, B. et al. (May 2022). "Cosmic-ray generated bubbles around their sources". In: MNRAS 512.1, pp. 233–244. DOI: 10.1093/mnras/stac466. arXiv: 2202.05814 [astro-ph.HE].

Bibliography III

Seo, Jeongbhin et al. (Apr. 2018). "The Contribution of Stellar Winds to Cosmic Ray Production". In: *Journal of Korean Astronomical Society* 51.2, pp. 37–48. DOI: 10.5303/JKAS.2018.51.2.37. arXiv: 1804.07486 [astro-ph.HE].

Watters, Kyle P. and Roger W. Romani (Feb. 2011). "The Galactic Population of Young gamma-ray Pulsars". In: ApJ 727.2, 123, p. 123. DOI: 10.1088/0004-637X/727/2/123. arXiv: 1009.5305 [astro-ph.HE].

Weaver, R. et al. (Dec. 1977). "Interstellar bubbles. II. Structure and evolution.". In: ApJ 218, pp. 377–395. DOI: 10.1086/155692.

Wright, Nicholas J. (Nov. 2020). "OB Associations and their origins". In: New A Rev. 90, 101549, p. 101549. DOI: 10.1016/j.newar.2020.101549. arXiv: 2011.09483 [astro-ph.SR].

Zinnecker, Hans and Harold W. Yorke (Sept. 2007). "Toward Understanding Massive Star Formation". In: ARA&A 45.1, pp. 481–563. DOI: 10.1146/annurev.astro.44.051905.092549. arXiv: 0707.1279 [astro-ph].

ISM model

Assumptions

- **Constant interstellar medium** around the CC SN
- Distributions of E_{SN} and n_{ISM}

ISM model

Assumptions

- **Constant interstellar medium** around the CC SN
- Distributions of E_{SN} and n_{ISM}

SNR evolution

Analytical solutions following Cioffi et al. (1988), compared with the calculator by Leahy and Williams (2017):

- Sedov-Taylor phase
- Pressure-Driven Snowplough phase
- (Momentum Conserving Stage)
- Merger with the ISM

ISM model: SN energy and ISM density

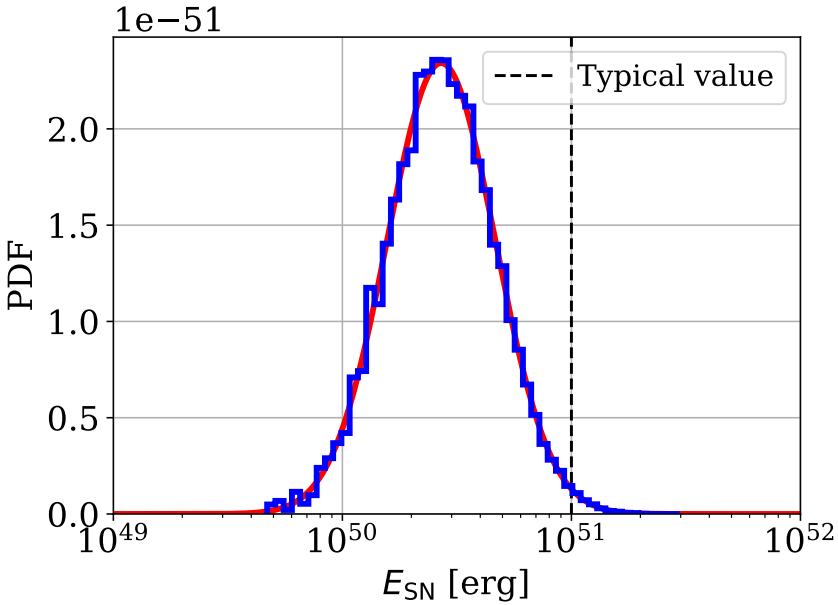

(a) Effective E_{SN} PDF, $\mu = 2.7 \times 10^{50}$ erg, $\sigma = 3.5$

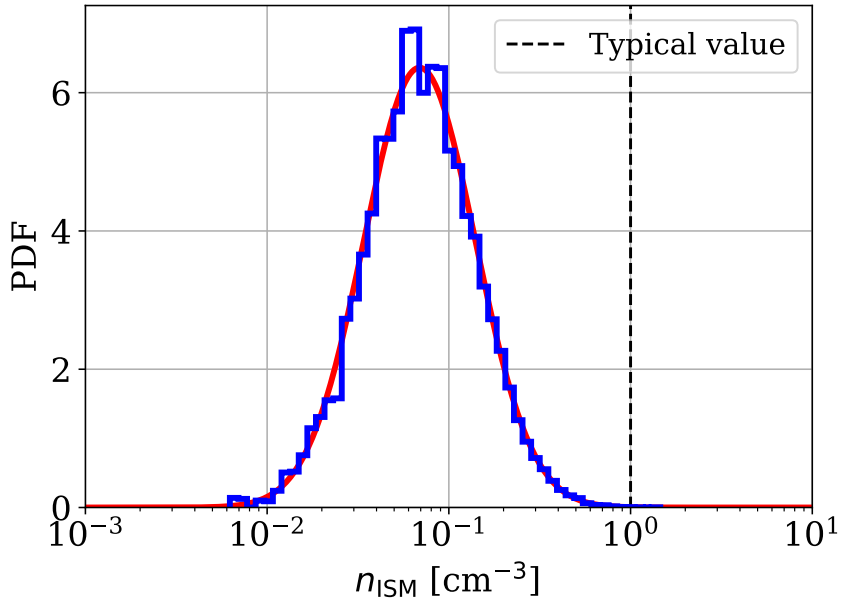

(b) Effective n_{ISM} PDF, $\mu = 0.069$ cm^{-3}, $\sigma = 5.1$

Figure: Lognormal distributions, following Leahy, Ranasinghe, et al. (2020). Computed by assuming a constant ISM density surrounding each of 43 SNe.

ISM model: Escape time

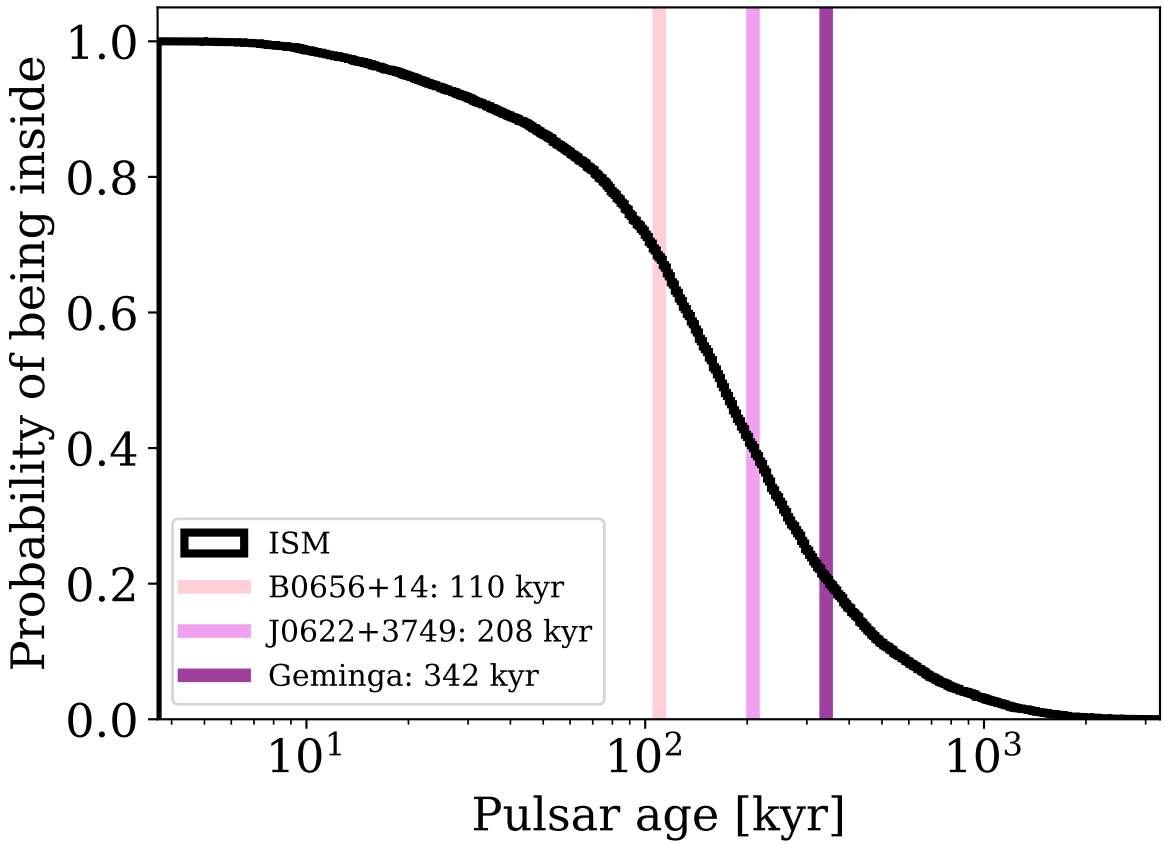

Figure: Probability of pulsars being inside the **SNR** as a function of time for the **ISM** model. Characteristic ages of pulsars are orders of magnitude, taken from the catalog of Manchester et al. (2005).

IMSB model: Comparing the shell mass and the SNR mass

Parameters for a star of $\mathbf{M_{ZAMS} = 8\ M_\odot}$

- Bubble radius $\mathbf{r_b = 20\ pc}$,
- Surrounding ISM density of $\mathbf{n_{ISM} = 1\ cm^{-3}}$,
- Mass lost in winds $\mathbf{\Delta M_{MS} = 0.1\ M_\odot}$ and $\mathbf{\Delta M_{RSG} = 3.4\ M_\odot}$,
- Ejecta mass is $M_{\rm ZAMS} - \Delta M_{\rm MS} - \Delta M_{\rm RSG} - M_{\rm pulsar} = \mathbf{M_{ej} = 3.1\ M_\odot}$,
- Mass swept in the bubble by the SNR is the mass lost in winds.

IMSB model: Comparing the shell mass and the SNR mass

Parameters for a star of $\mathbf{M_{ZAMS} = 8\ M_\odot}$

- Bubble radius $\mathbf{r_b = 20\ pc}$,
- Surrounding ISM density of $\mathbf{n_{ISM} = 1\ cm^{-3}}$,
- Mass lost in winds $\mathbf{\Delta M_{MS} = 0.1\ M_\odot}$ and $\mathbf{\Delta M_{RSG} = 3.4\ M_\odot}$,
- Ejecta mass is $M_{ZAMS} - \Delta M_{MS} - \Delta M_{RSG} - M_{pulsar} = \mathbf{M_{ej} = 3.1\ M_\odot}$,
- Mass swept in the bubble by the SNR is the mass lost in winds.

Computations

$$M_{shell} = \frac{4\pi}{3} \rho_{ISM} r_b^3 = 755\ M_\odot \quad (2)$$

Mass ratio:

$$\frac{M_{shell}}{M_{ej} + \Delta M} = 116 \quad (3)$$

Shell stops the expansion of the SNR

IMSB model: Comparing the shell mass and the SNR mass

Parameters for a star of $\mathbf{M_{ZAMS} = 8\ M_\odot}$

- Bubble radius $\mathbf{r_b = 20\ pc}$,
- Surrounding ISM density of $\mathbf{n_{ISM} = 1\ cm^{-3}}$,
- Mass lost in winds $\mathbf{\Delta M_{MS} = 0.1\ M_\odot}$ and $\mathbf{\Delta M_{RSG} = 3.4\ M_\odot}$,
- Ejecta mass is $M_{ZAMS} - \Delta M_{MS} - \Delta M_{RSG} - M_{pulsar} = \mathbf{M_{ej} = 3.1\ M_\odot}$,
- Mass swept in the bubble by the SNR is the mass lost in winds.

Computations

$$M_{shell} = \frac{4\pi}{3} \rho_{ISM} r_b^3 = 755\ M_\odot \quad (2)$$

Mass ratio:

$$\frac{M_{shell}}{M_{ej} + \Delta M} = 116 \quad (3)$$

Shell stops the expansion of the SNR

Conclusion

Boundary: bubble radius instead of the SNR

IMSB model

Theoretical framework for the SNR shock

Time (Numerically integrated)

$$t(R_s) = \int_0^{R_s} \frac{1}{u_s(r)} \mathrm{d}r \tag{4}$$

Speed (Analytical)

$$u_s(R_s) = \frac{\gamma + 1}{2} \left[\frac{2\alpha E_{SN}}{M^2(R_s) R_s^{\alpha}} \times \int_0^{R_s} r^{\alpha - 1} M(r) \mathrm{d}r \right] \tag{5}$$

with $\alpha = 6(\gamma - 1)/(\gamma + 1)$.

Mass (Analytical)

$$M(r) = M_{ej} + 4\pi \int_0^{r} r'^2 \rho(r') \mathrm{d}r' \tag{6}$$

The numbers (model from Weaver et al. (1977))

Wind region ($R_s < r_w$):

$$\rho_w(R_s) = \frac{\dot{M}}{4\pi u_w R_s^2}$$

Bubble region ($r_w < R_s < r_b$):

$$\rho_b(R_s) = \rho_b$$

Shell region ($r_b < R_s < r_{ISM}$):

$$\rho_{shell} = \frac{M_{shell}}{V_{shell}} = \frac{\frac{4\pi}{3} r_b^3 \rho_{ISM}}{\frac{4\pi}{3}\left(r_{ISM}^3 - r_b^3\right)}$$

ISM region ($r_{ISM} < R_s$):

$$\rho_{ISM} = 1 \text{ cm}^{-3}$$

IMSB model

Looking at all the distributions

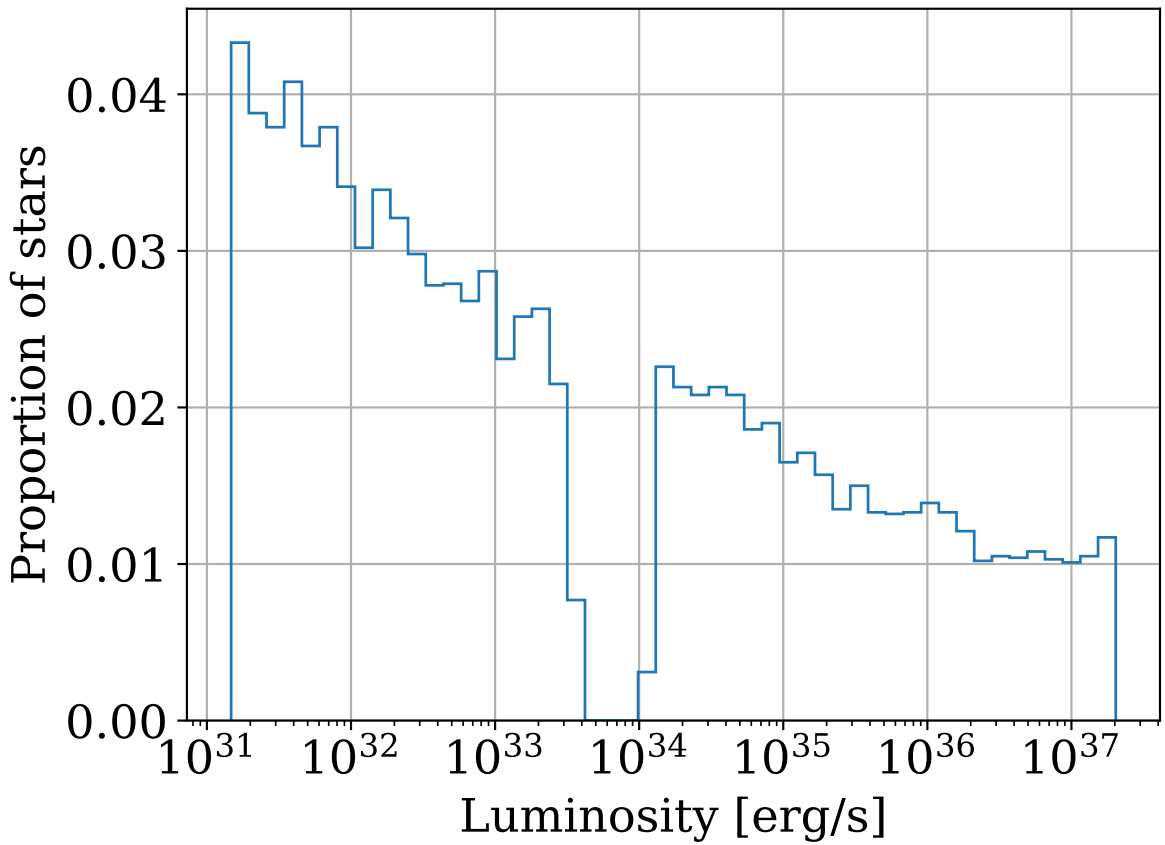

Figure: Luminosity distribution.

IMSB model

Looking at all the distributions

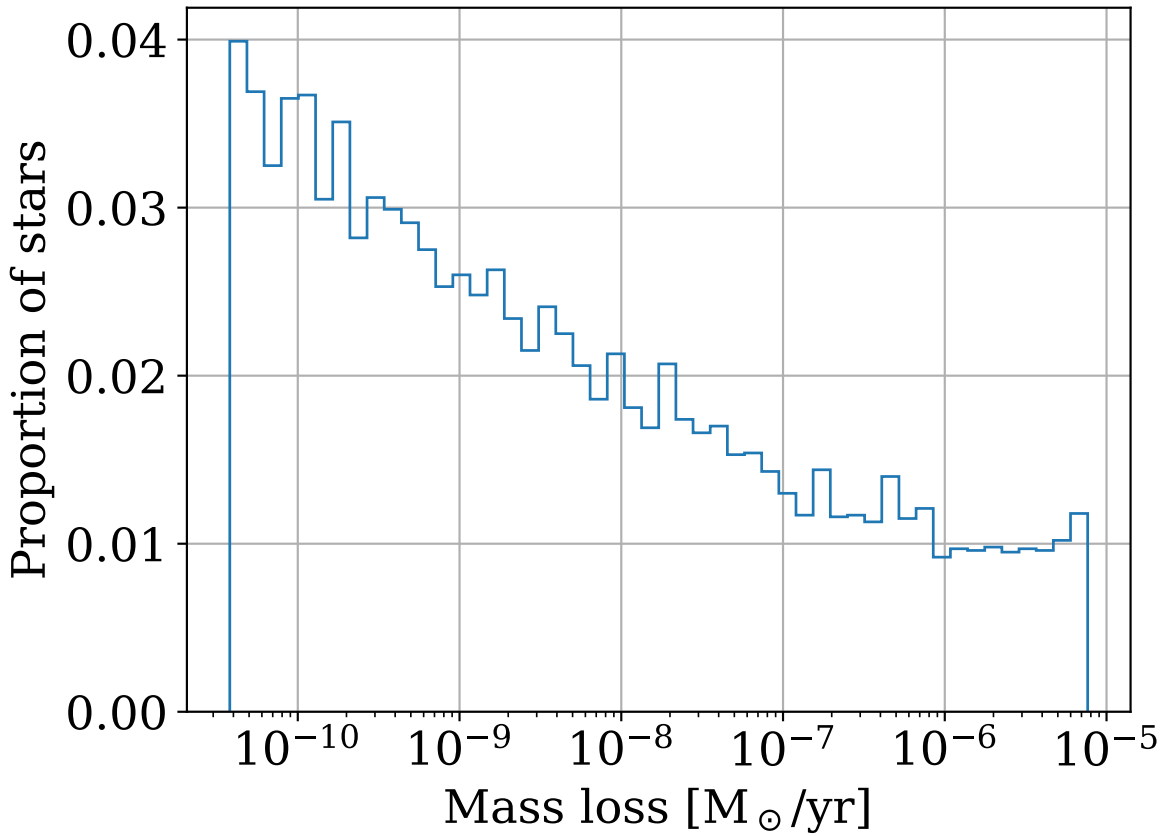

Figure: Mass loss distribution.

IMSB model

Looking at all the distributions

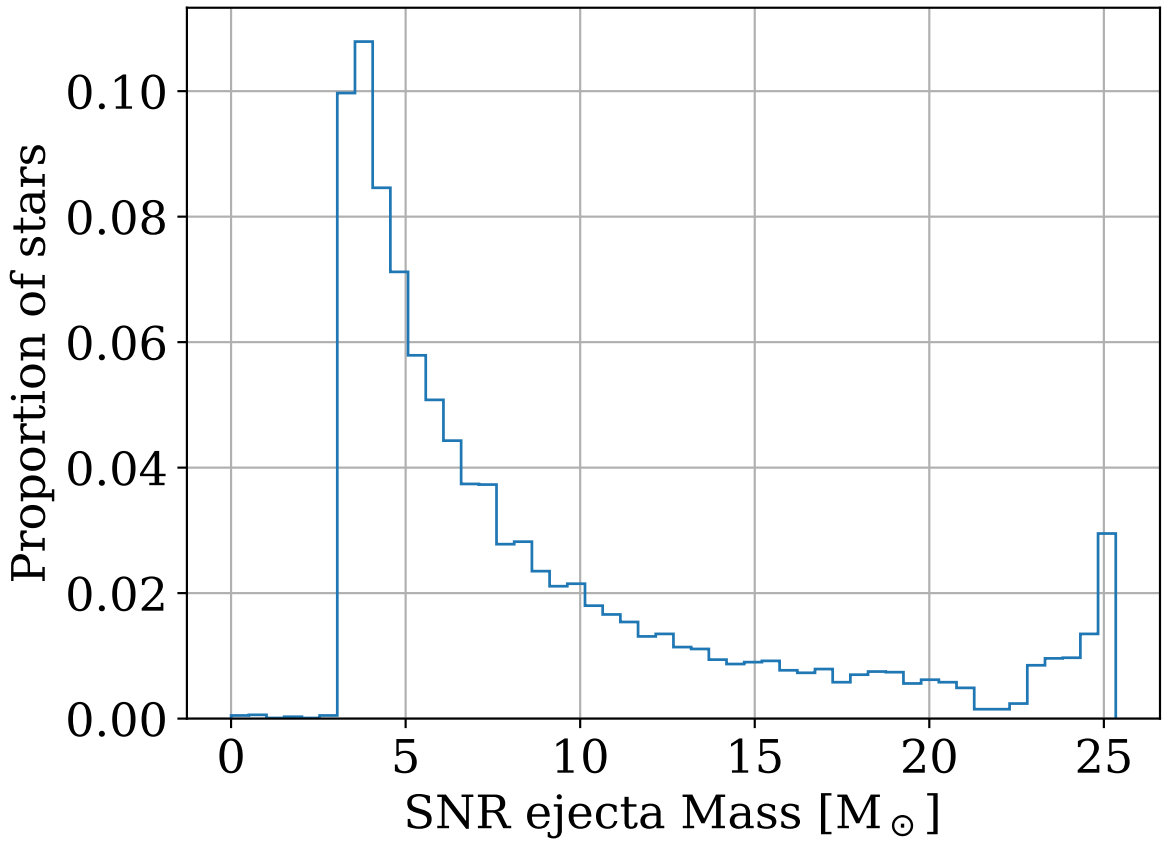

Figure: SNR ejecta mass distribution.

IMSB model

Looking at all the distributions

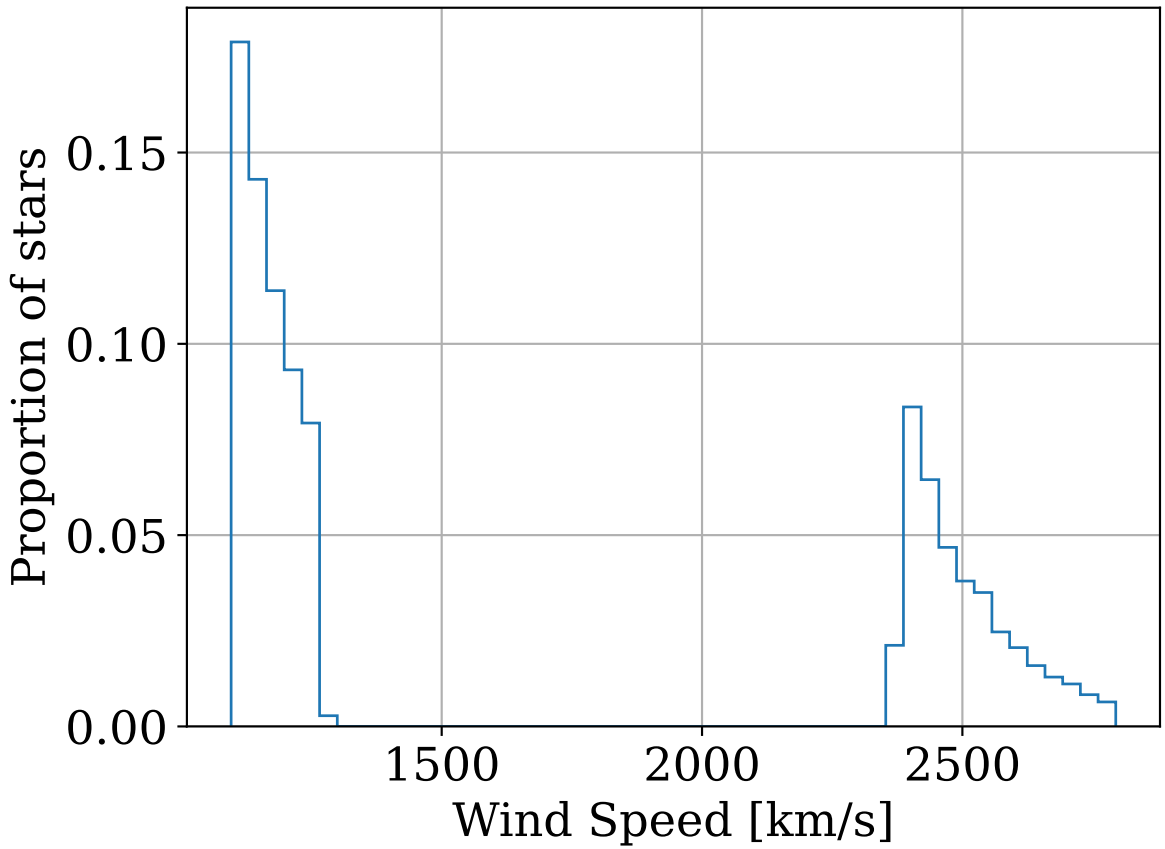

Figure: Wind speed distribution.

IMSB model

Looking at all the distributions

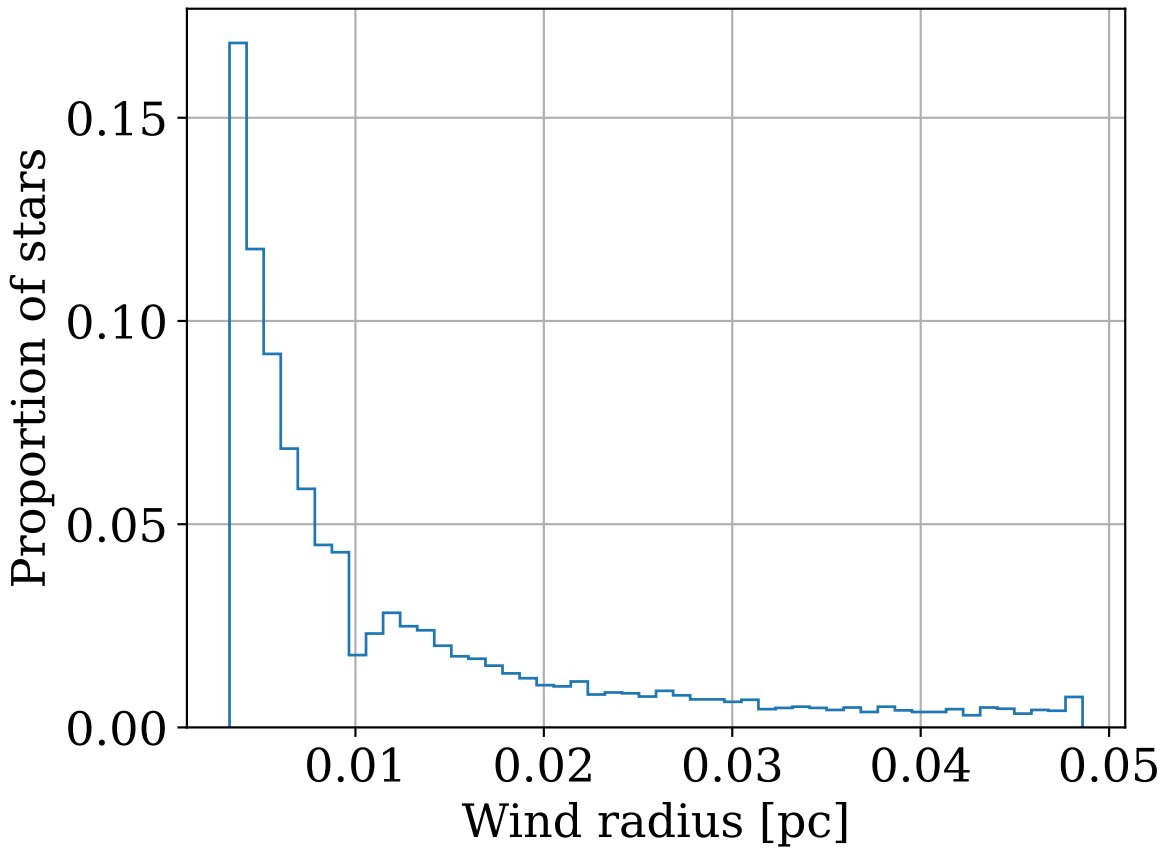

Figure: Wind radius distribution.

IMSB model

Looking at all the distributions

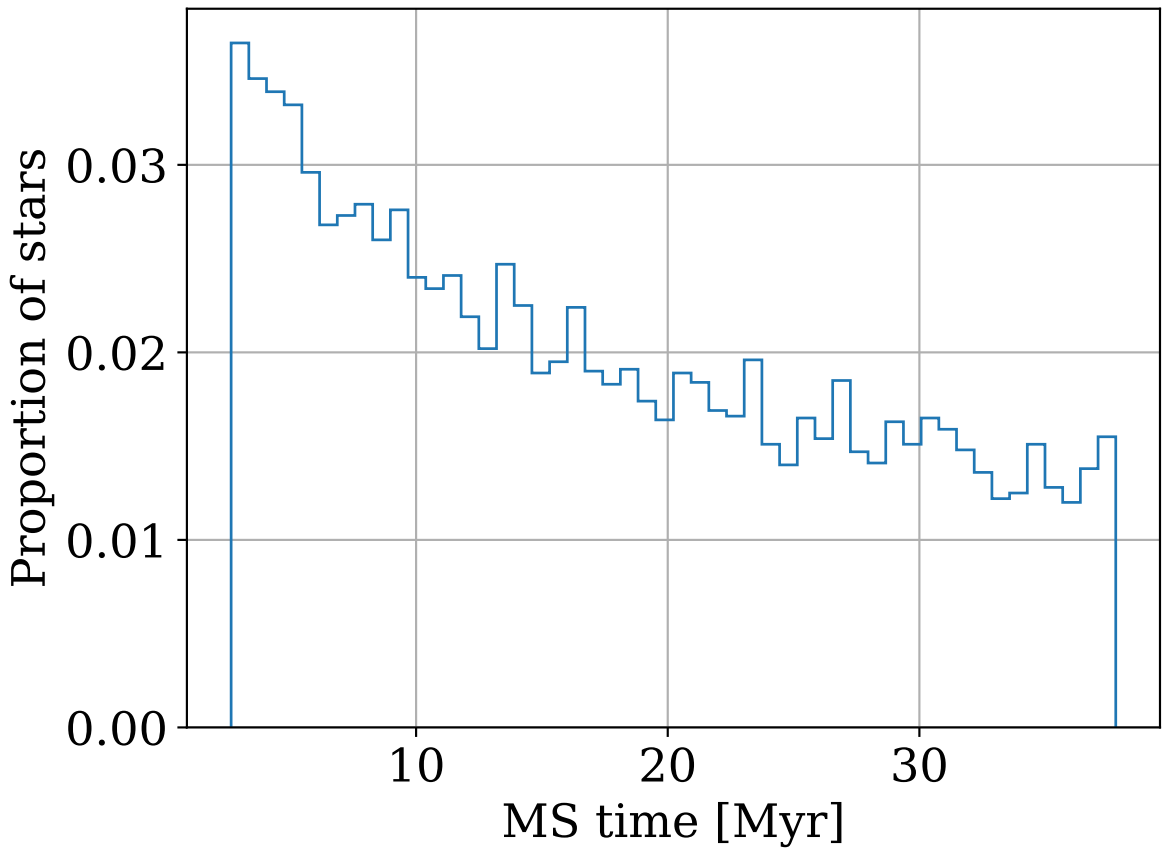

Figure: Main sequence time distribution.

IMSB model

Looking at all the distributions

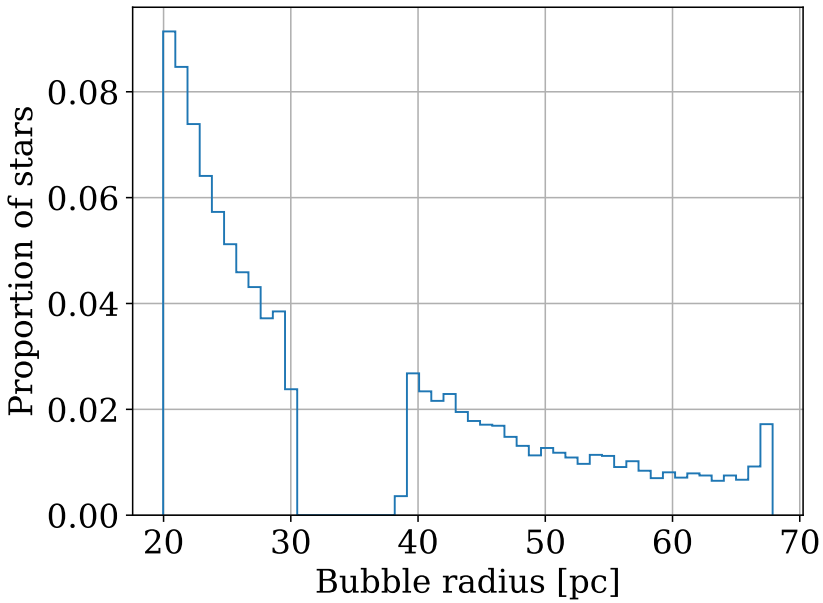

Figure: Bubble radius distribution.

Formula

From Weaver et al. (1977) and Härer et al. (2023):

$$r_{\mathrm{b}} = 21 \text{ pc } \zeta_{\mathrm{b}}^{1/5} L_{36}^{1/5} n_{\mathrm{ISM},1}^{-1/5} t_6^{3/5} \quad (7)$$

IMSB model

Looking at all the distributions

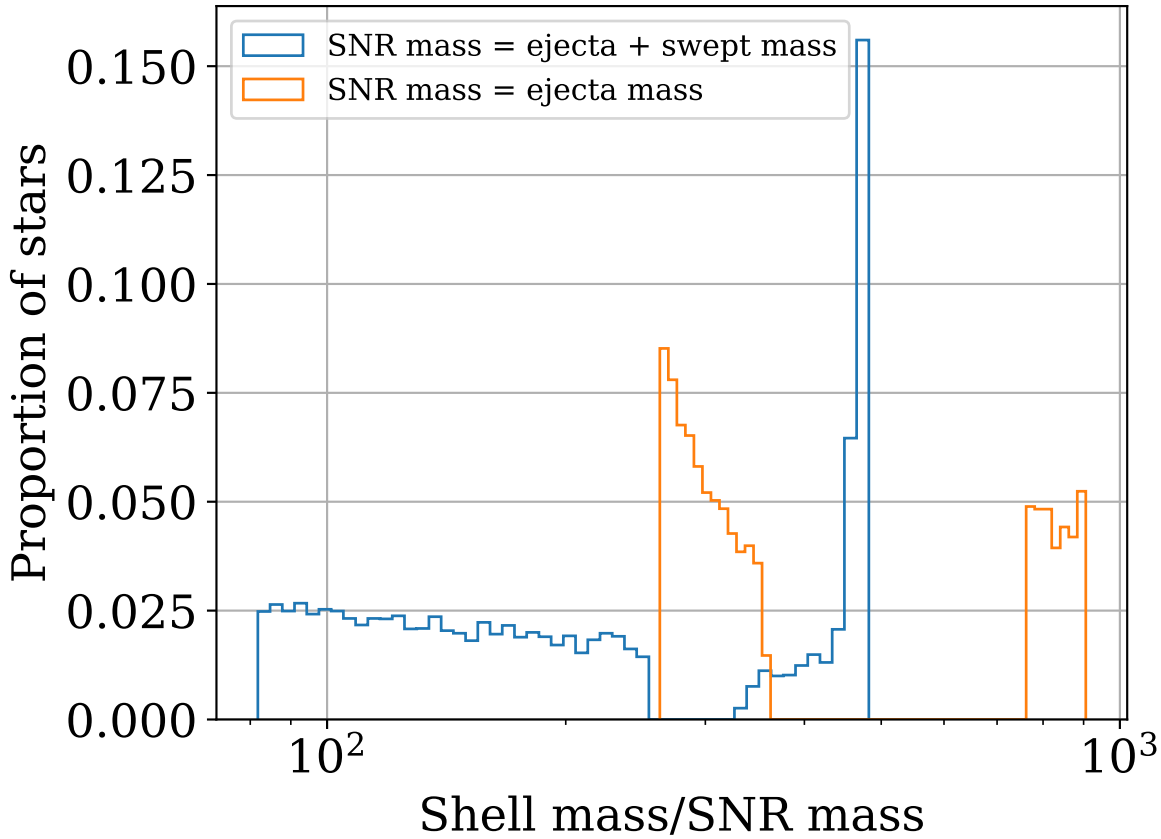

Figure: Shell mass/SNR mass distribution. We show for both the ejecta mass and the swept mass. Naturally, the swept mass is higher than the ejecta mass, resulting in a lower (by less than an order of magnitude) ratio. The shape in two parts of the orange curve is linked to the shape of the bubble radius (which is the determining factor for the parameter).

IMSB model

Density profile

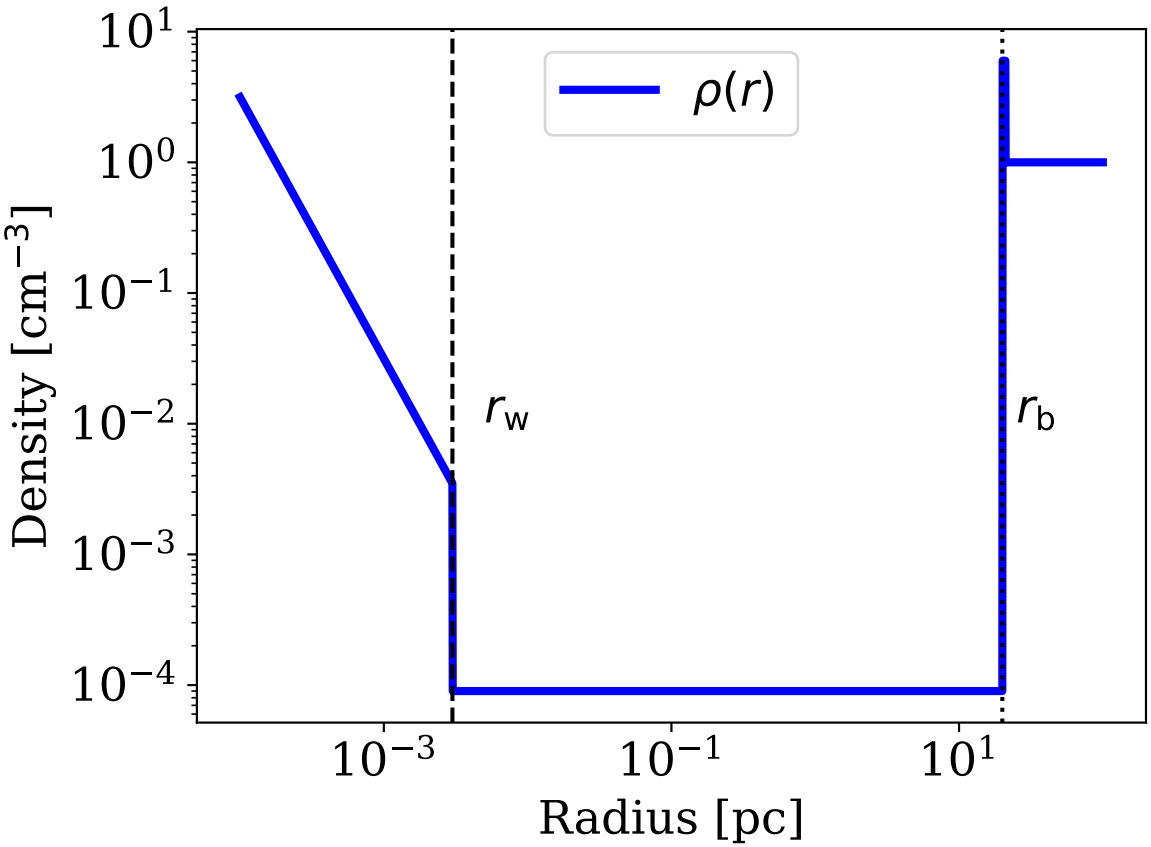

Figure: Density profile in the IMSB, based on Weaver et al. (1977).

IMSB model

Mass profile

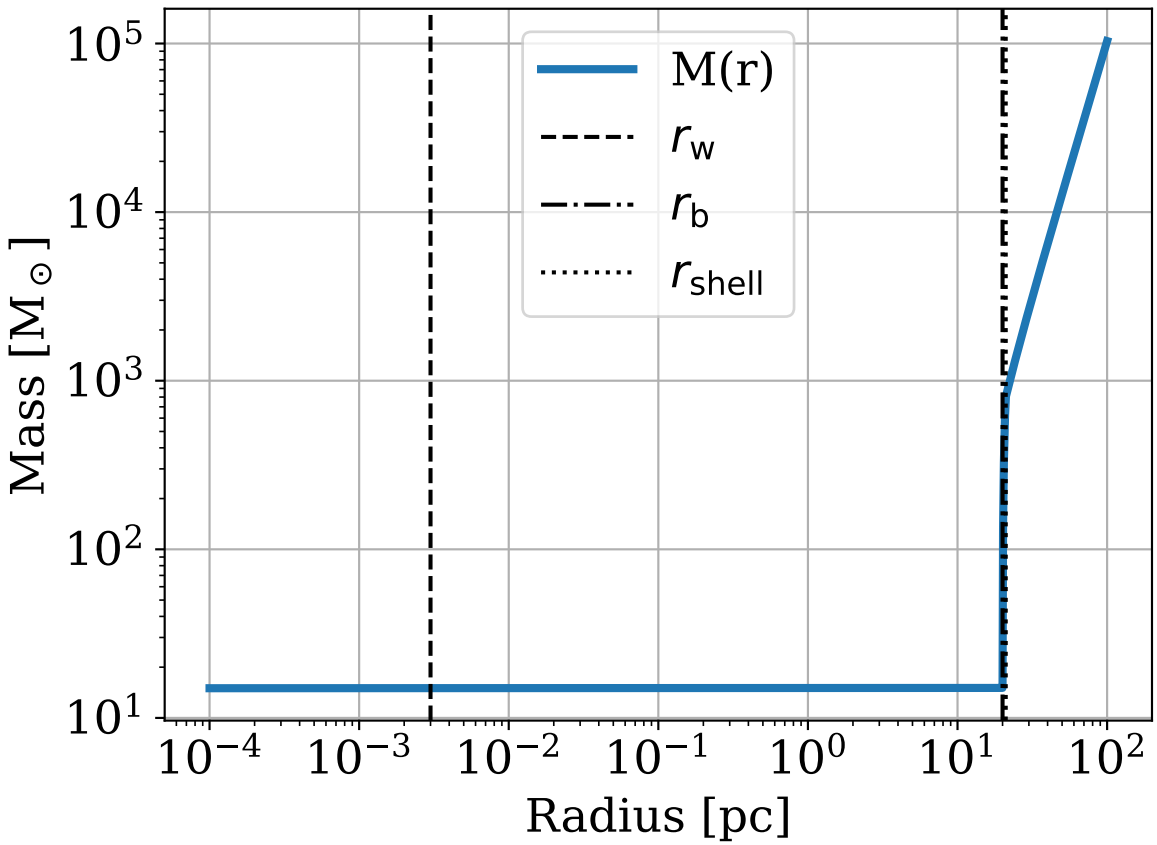

Figure: Accumulated mass profile in the IMSB, analytically computed from the density profile

IMSB model

Speed profile

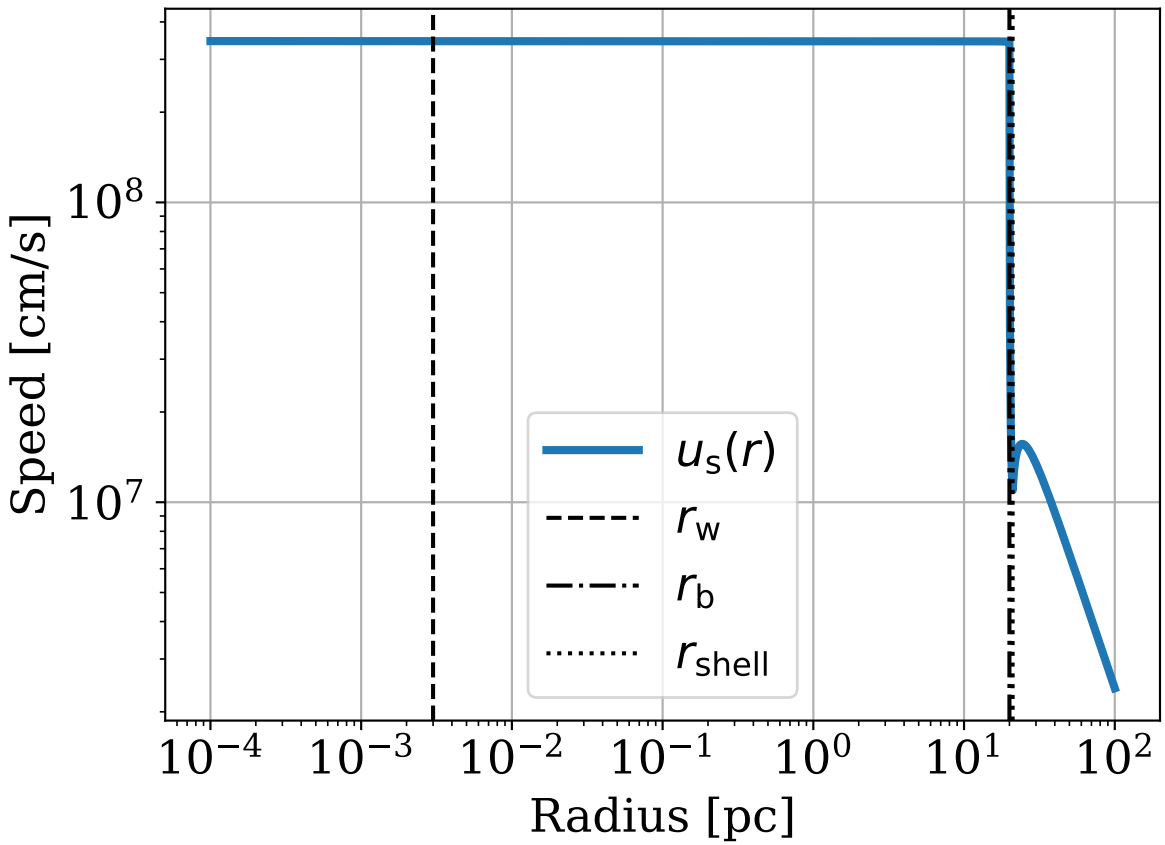

Figure: Accumulated speed profile in the IMSB, analytically computed from the mass profile

Radiative pha se

$$t_{\text{rad}} = \frac{3}{2}\frac{k_b T}{n\Lambda(T)}$$

with $\Lambda(T) = 1.6 \times 10^{-19}\ T^{-1/2}$ erg/cm^3/s. We always go radiative when reaching the shell.

Merger with the bubble shell

$$u_s(R_s) = \beta c_{\text{sound}}(T(R_s))$$

with $\beta = 3$ and the speed of sound c_{sound} depending on the temperature profile found in Weaver et al. (1977). Since the SNR stops inside the shell, it merges there.

SB model

Looking at all the distributions

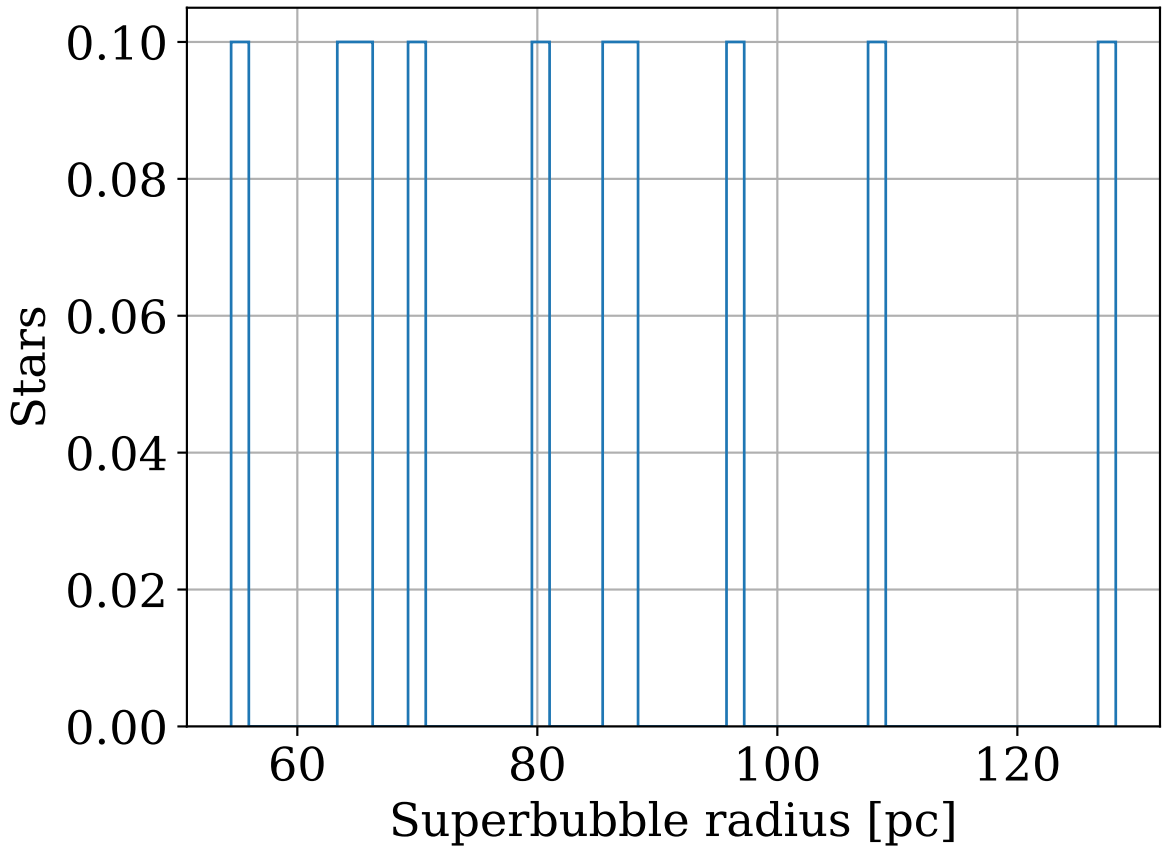

Figure: Superbubble radius distribution.

Comparing the probability of being inside the boundary

Special case: exiting the SNR inside the bubble

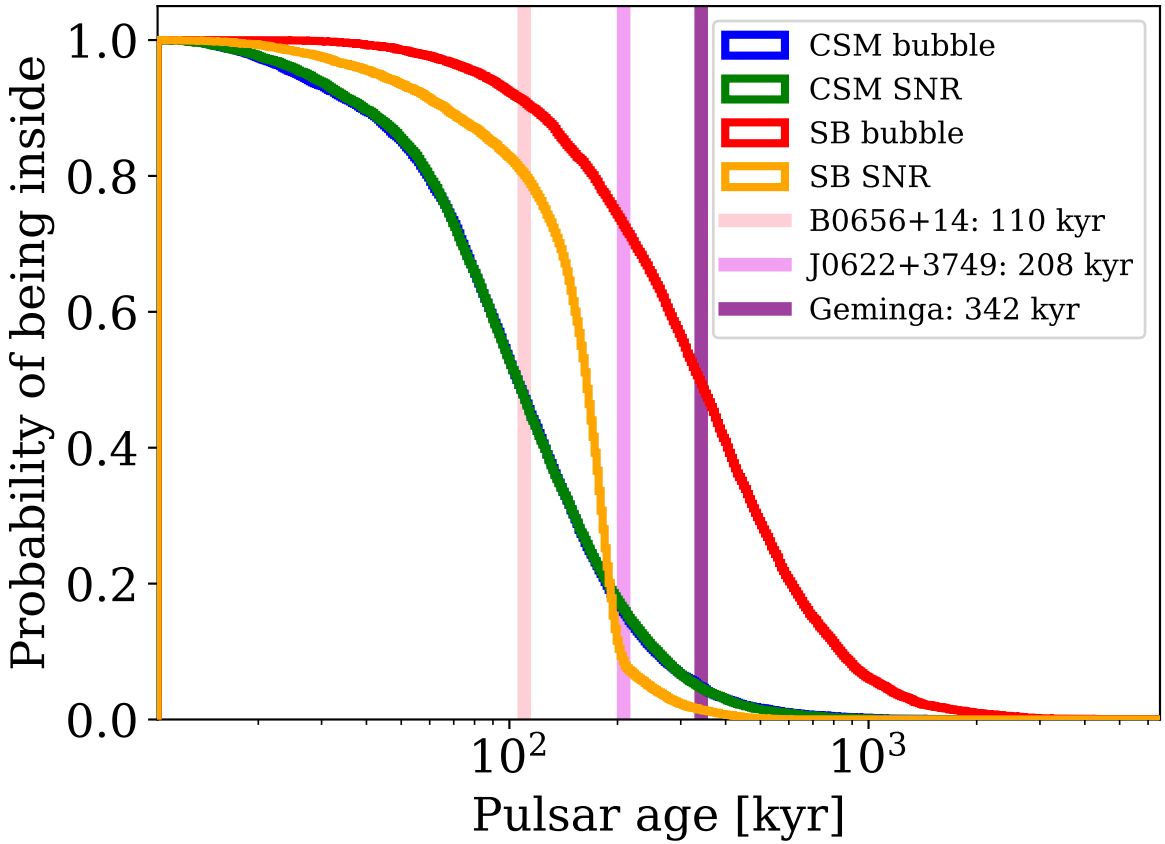

Figure: Probability of pulsars being inside the **bubble (SB)** as a function of time for the **IMSB (SB)** models respectively. Max mass 40 $M_\odot$.
The green curve corresponds to the escape time of pulsars from the SNR inside the IMSB, and the orange inside the SB.

Energy available for escaping pulsars

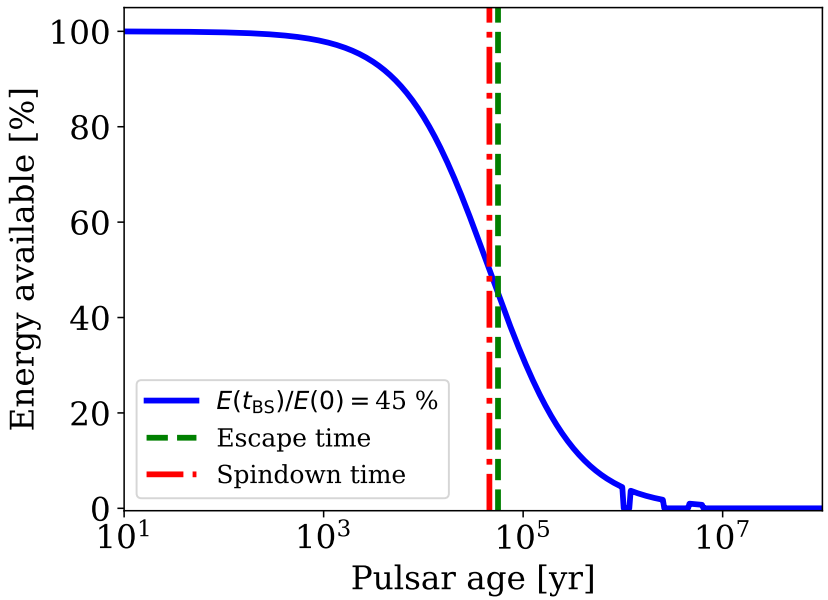

Figure: Evolution of the available energy of a pulsar as a function of time. Towards the later ages there are integration artifacts. $P_0 = 100$ ms, $v_k = 280$ km/s as in Evoli, Amato, et al. (2021).

Energy available for escaping pulsars

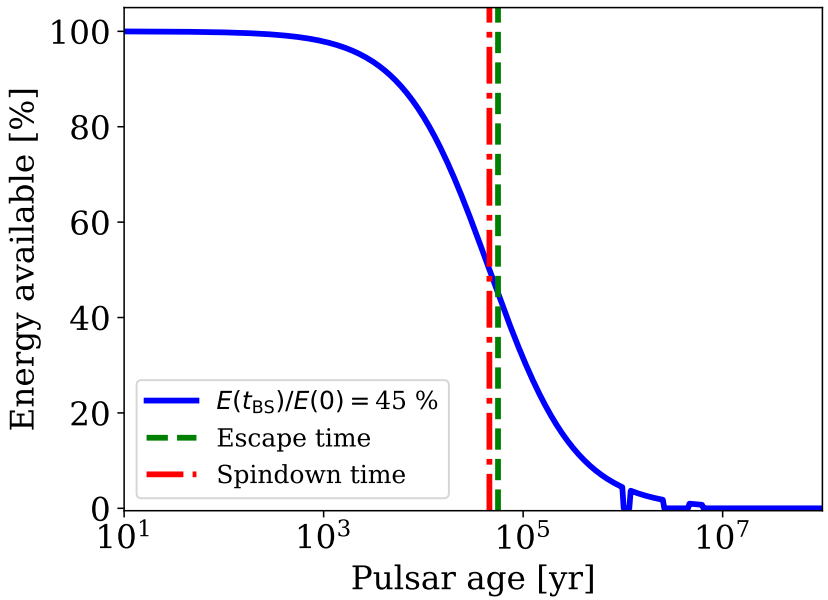

Figure: Evolution of the available energy of a pulsar as a function of time. Towards the later ages there are integration artifacts. $P_0 = 100$ ms, $v_k = 280$ km/s as in Evoli, Amato, et al. (2021).

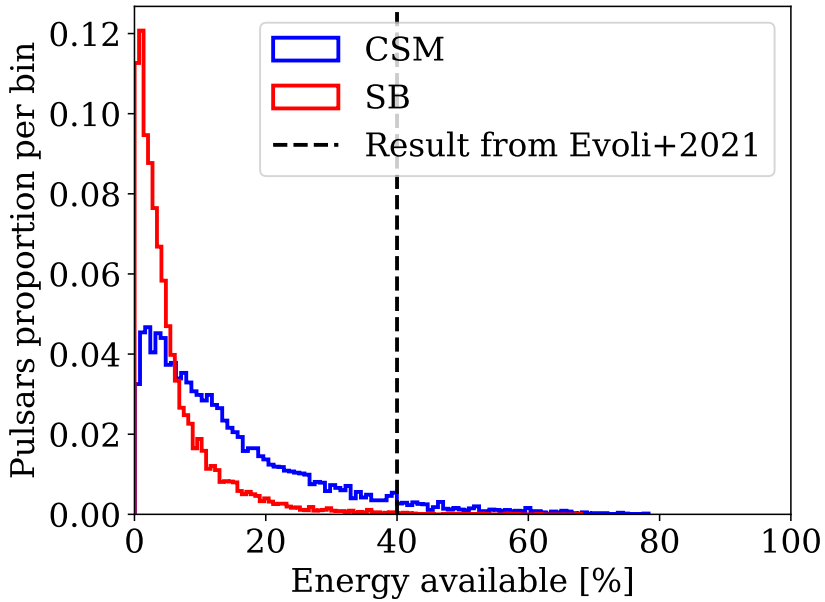

Figure: Distribution of available energies after escape. The initial period distribution comes from γ-ray observations in Watters et al. (2011).

Energy available for escaping pulsars

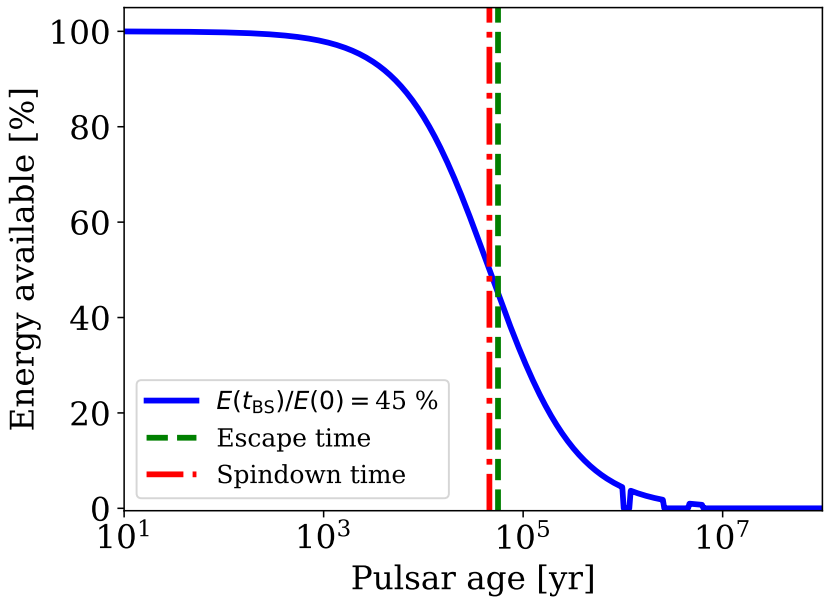

Figure: Evolution of the available energy of a pulsar as a function of time. Towards the later ages there are integration artifacts.
$P_0 = 100$ ms, $v_k = 280$ km/s as in Evoli, Amato, et al. (2021).

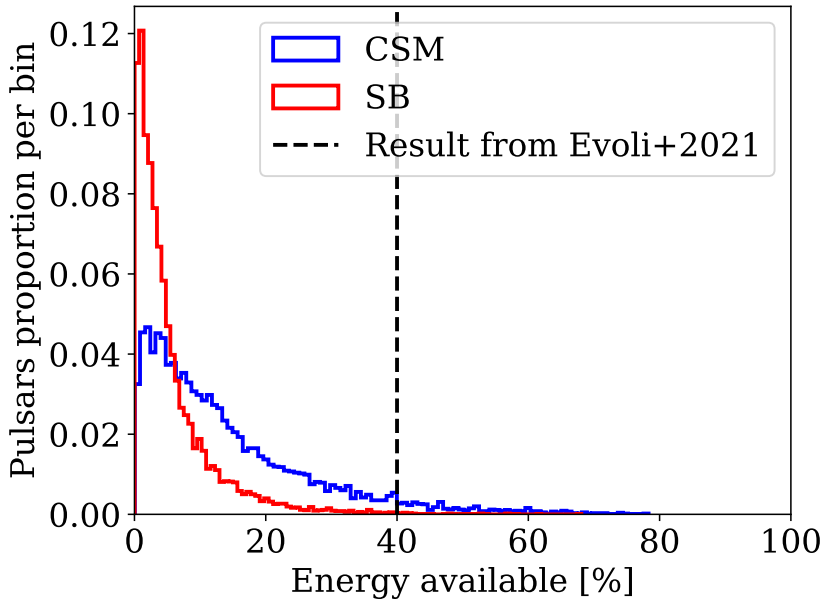

Figure: Distribution of available energies after escape. The initial period distribution comes from γ-ray observations in Watters et al. (2011).
Pulsars **DO NOT** have much energy left + leptons represent only a percentage of this energy